nature astronomy

SUPPLEMENTARY INFORMATION

https://doi.org/10.1038/s41550-017-0325-8

In the format provided by the authors and unedited.

Constraints on the spin evolution of young planetary-mass companions

Marta L. Bryan[1]*, Björn Benneke[2], Heather A. Knutson[2], Konstantin Batygin[2] and Brendan P. Bowler[3]

[1]Cahill Center for Astronomy and Astrophysics, California Institute of Technology, Pasadena, CA, USA. [2]Division of Geological and Planetary Sciences, California Institute of Technology, Pasadena, CA, USA. [3]McDonald Observatory and Department of Astronomy, University of Texas at Austin, Austin, TX, USA. *e-mail: mlbryan@astro.caltech.edu

Supplementary Information

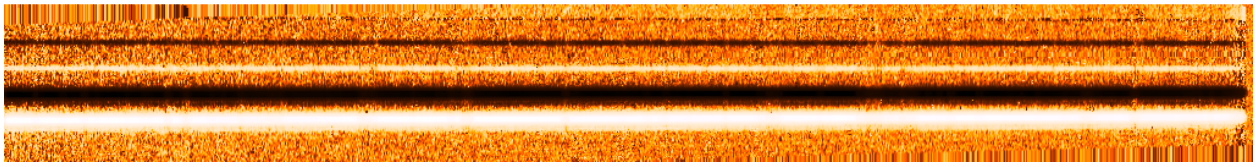

Supplementary Figure 1. Representative 2D rectified spectrum. 2D rectified order 1 spectrum for the system VHS 1256-1257. Both the stellar and planetary traces are visible in this spectrum.

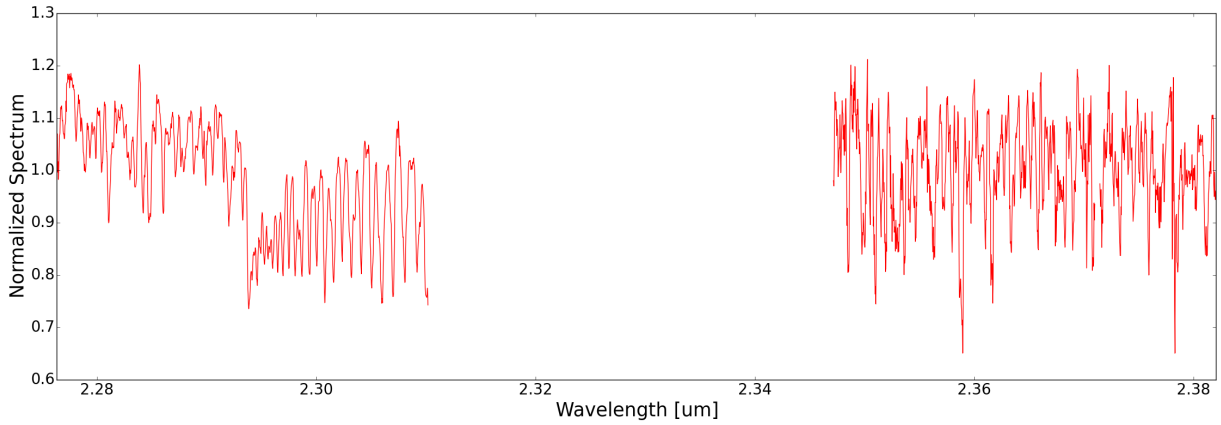

Supplementary Figure 2. Representative wavelength calibrated and telluric corrected spectrum. Orders 1 and 2 of the telluric-corrected spectrum for 2M0355+1133 dataset. Note the start of the CO bandhead at ~2.29 μm.

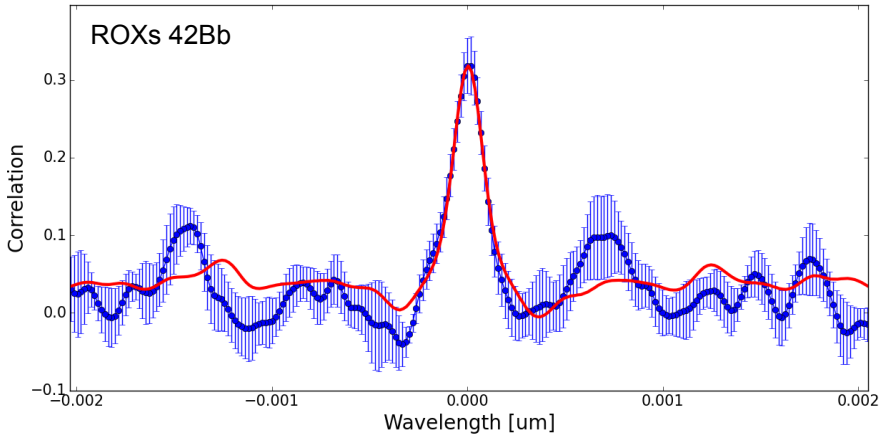

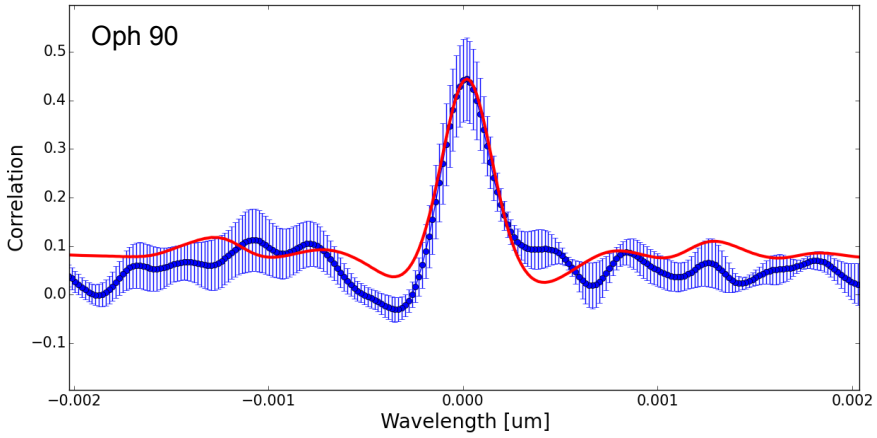
Oph 90
Correlation
Wavelength [um]

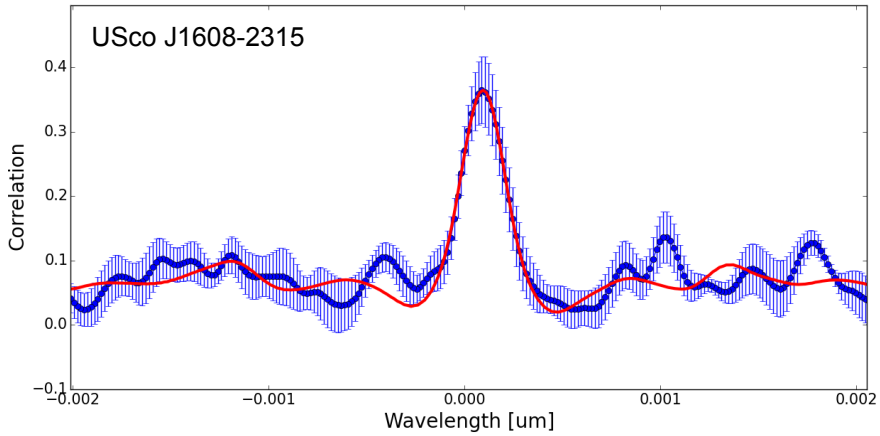
USco J1608-2315
Correlation
Wavelength [um]

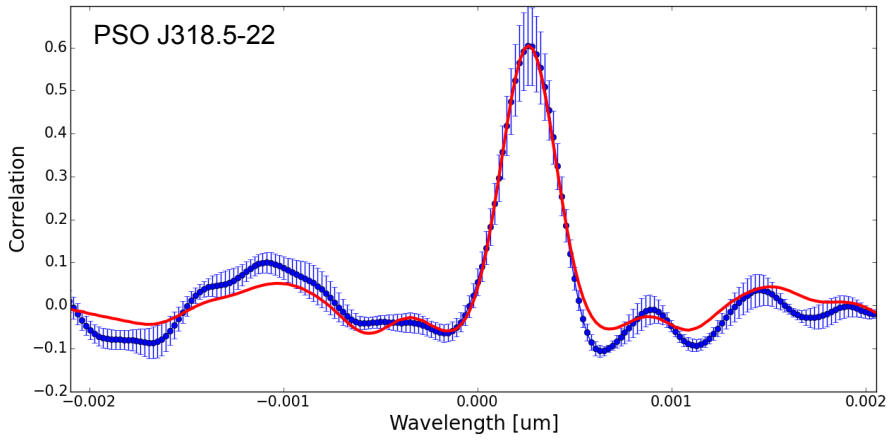
PSO J318.5-22
Correlation
Wavelength [um]

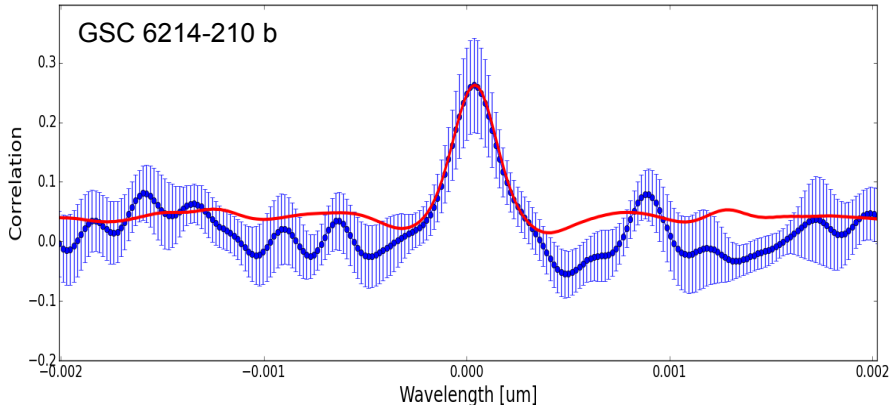
GSC 6214-210 b
Correlation
Wavelength [um]

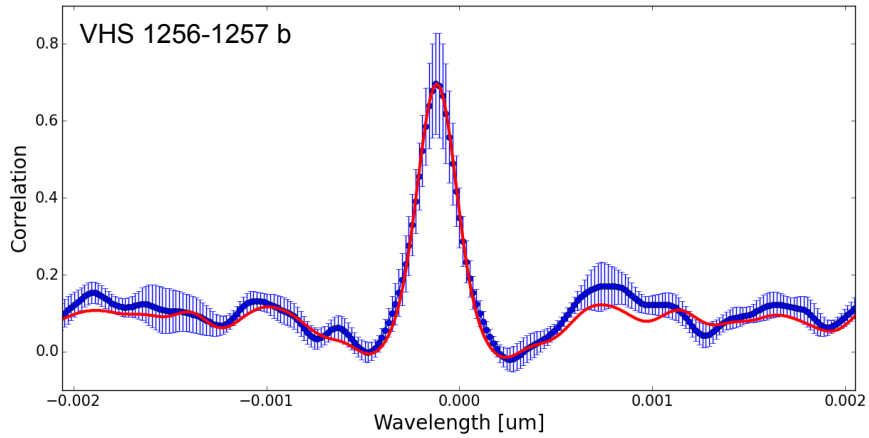
VHS 1256-1257 b
Correlation
Wavelength [um]

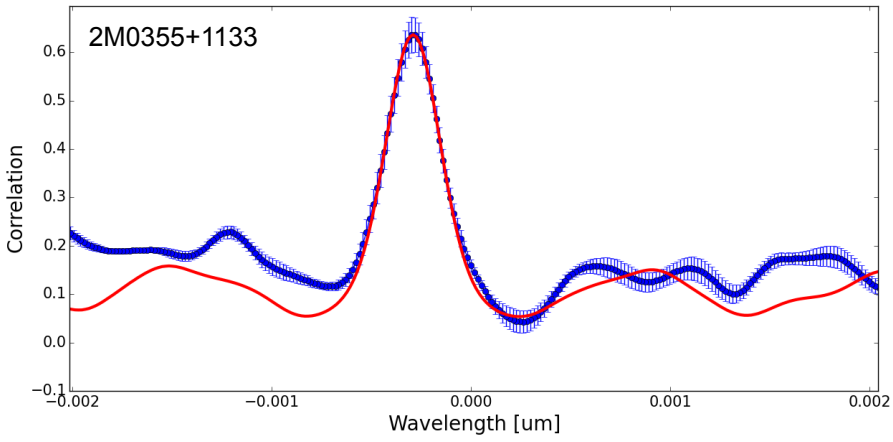
2M0355+1133
Correlation
Wavelength [um]

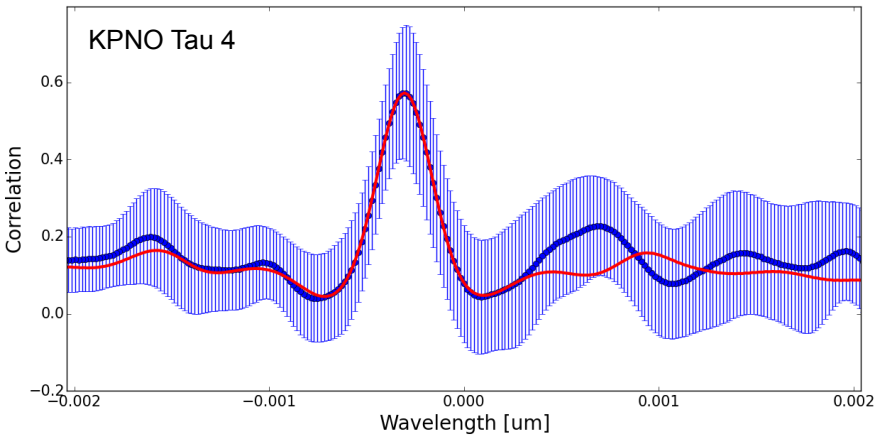

Supplementary Figure 3. Cross correlation functions for planetary-mass companions and low-mass brown dwarfs obtained from our NIRSPEC observations. Cross correlation functions for each object are plotted in blue, with the best-fit model overplotted in red. 1σ uncertainties on these CCFs are calculated using the jackknife resampling technique (see Methods section 3).

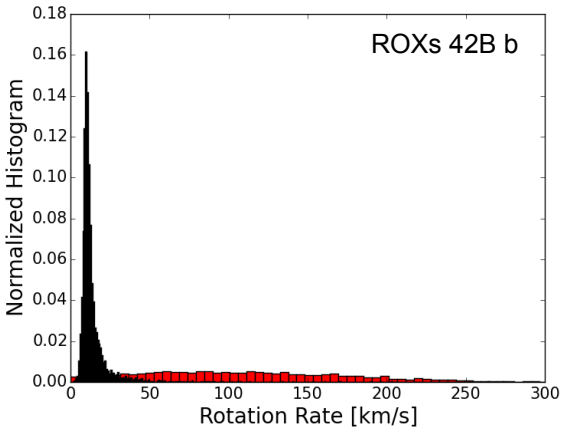
ROXs 42B b
Normalized Histogram
Rotation Rate [km/s]

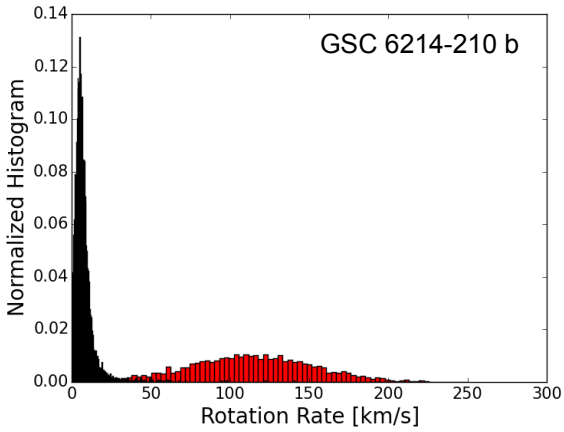
GSC 6214-210 b
Normalized Histogram
Rotation Rate [km/s]

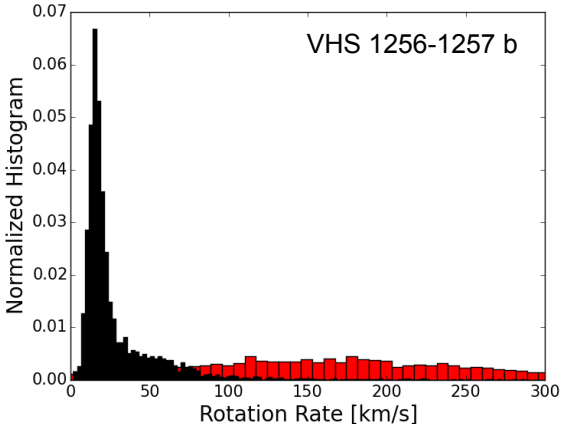
VHS 1256-1257 b
Normalized Histogram
Rotation Rate [km/s]

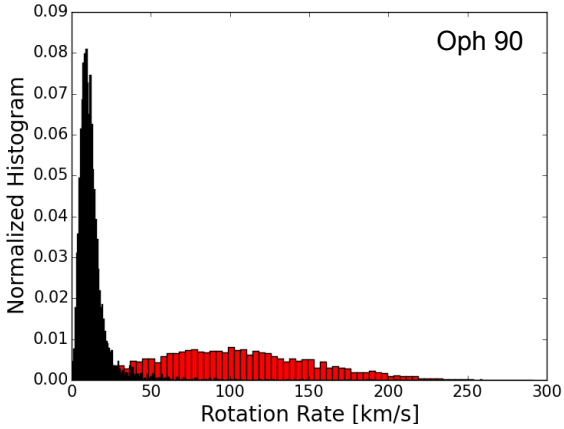
Oph 90
Normalized Histogram
Rotation Rate [km/s]

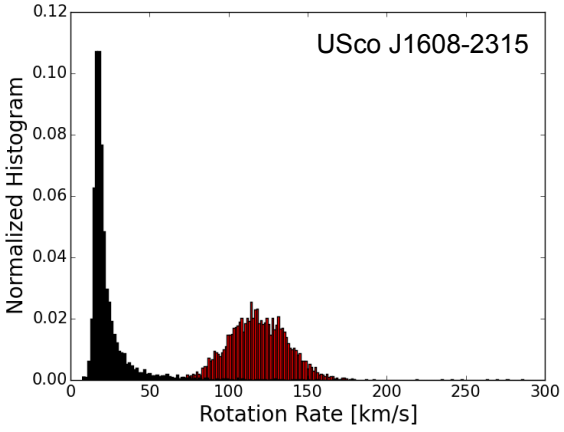
USco J1608-2315
Normalized Histogram
Rotation Rate [km/s]

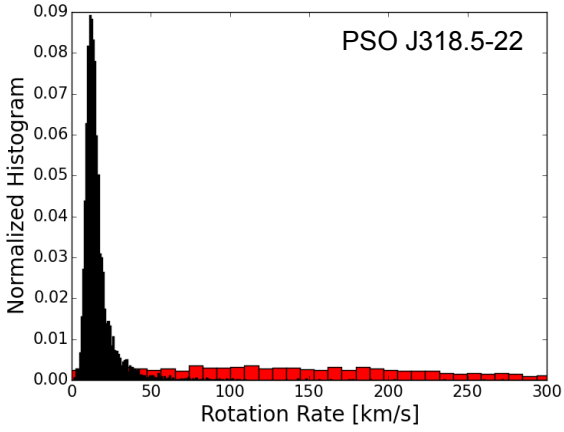
PSO J318.5-22
Normalized Histogram
Rotation Rate [km/s]

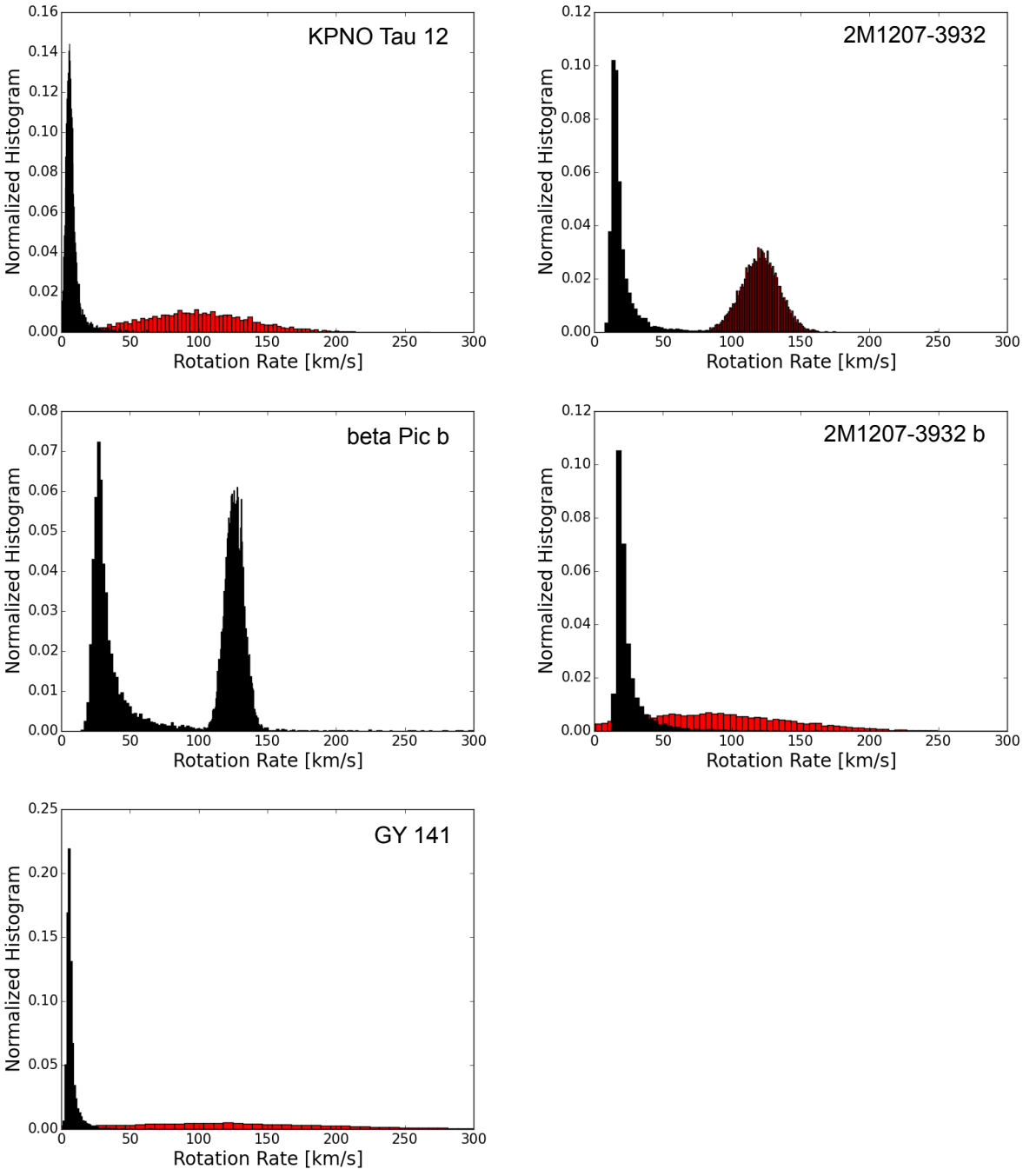

Supplementary Figure 4. Distributions of measured rotation rates and calculated break-up velocities for each object. The rotation rate distributions (black) have widths that are set by the uncertainties in the measured rotational line broadening and unknown inclination, and the break-up velocity distributions (red) typically have larger uncertainties that are set by errors in the estimated masses, ages, and radii.

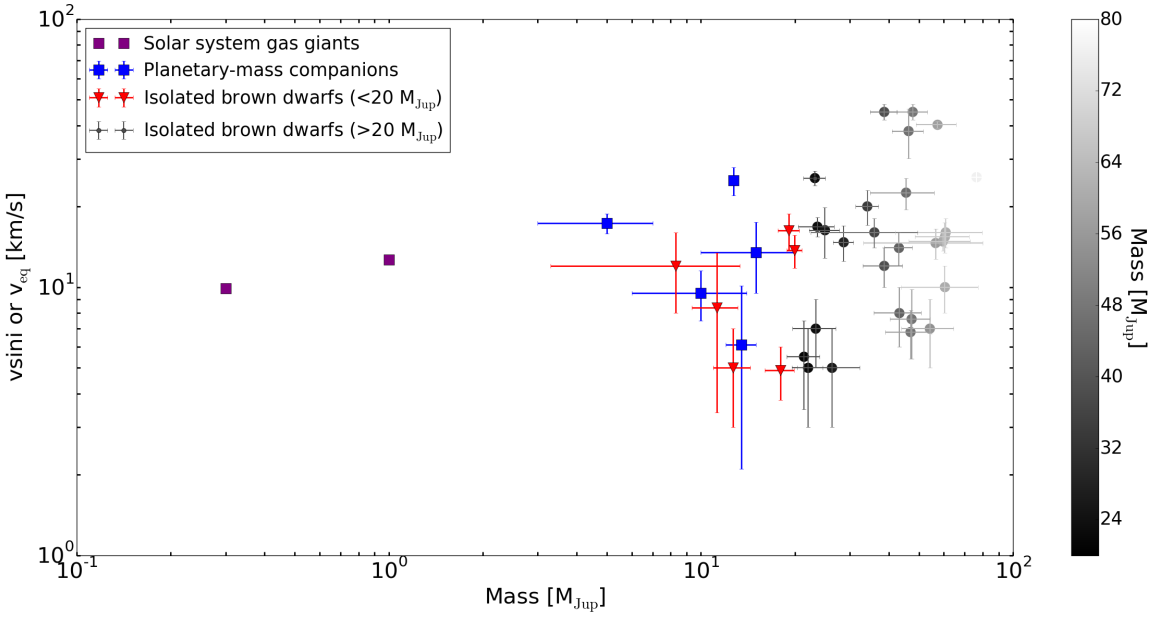

Supplementary Figure 5. No correlation between mass and rotation rate for masses less than 20 M_{Jup}. Here we show rotation rate measurements and corresponding 1σ uncertainties for the bound planetary-mass companion sample in blue and the isolated brown dwarf (<20 M_{Jup}) sample in red. We include the gas giant solar system planets as purple squares for reference. The rates for the brown dwarfs and all planetary-mass companions except for 2M1207-3932 b are projected velocities, and the rotation rates for 2M1207-3932 b and the solar system gas giants are equatorial velocities. We also plot rotation rate measurements for more massive brown dwarfs (20-80 M_{Jup}) as filled grey circles, with the shading indicating the mass of each object. Five of these measurements are equatorial velocities derived from photometric rotation periods and the rest are projected rotation rates from measurements of rotational line broadening.

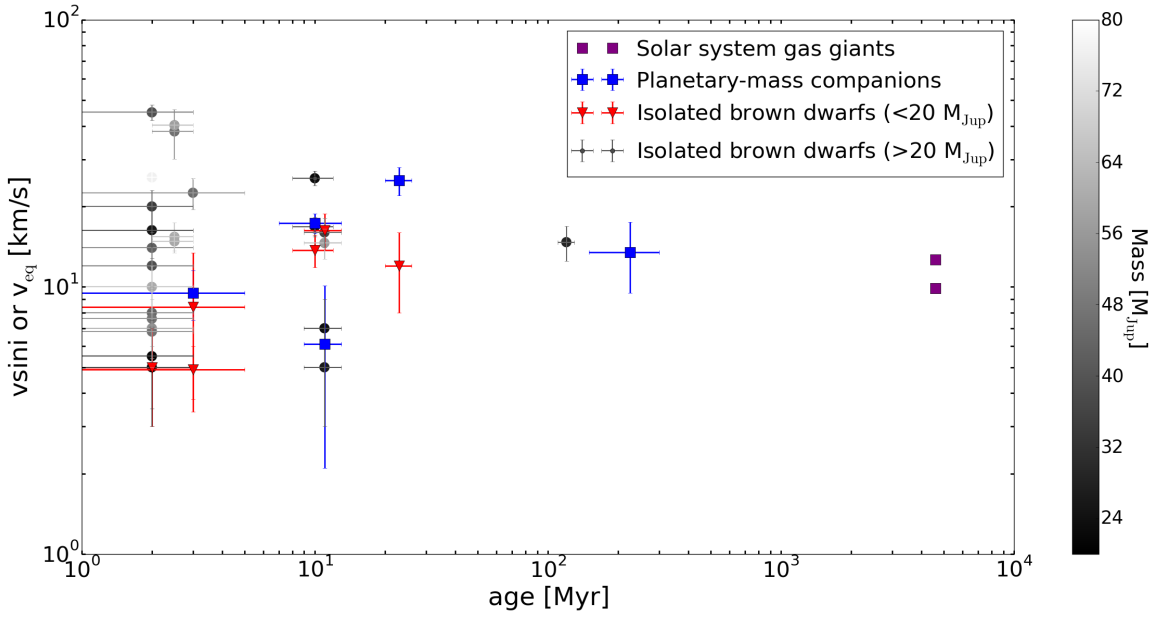

Supplementary Figure 6. Rotation rate measurements versus age for planetary-mass companions (blue squares) and brown dwarfs with masses less than 20 M_{Jup} (red triangles). We include the gas giant solar system planets as purple squares and show more massive (20-80 M_{Jup}) brown dwarfs as filled circles, where color shade of grey indicates the mass. 1σ uncertainties are shown for each object.

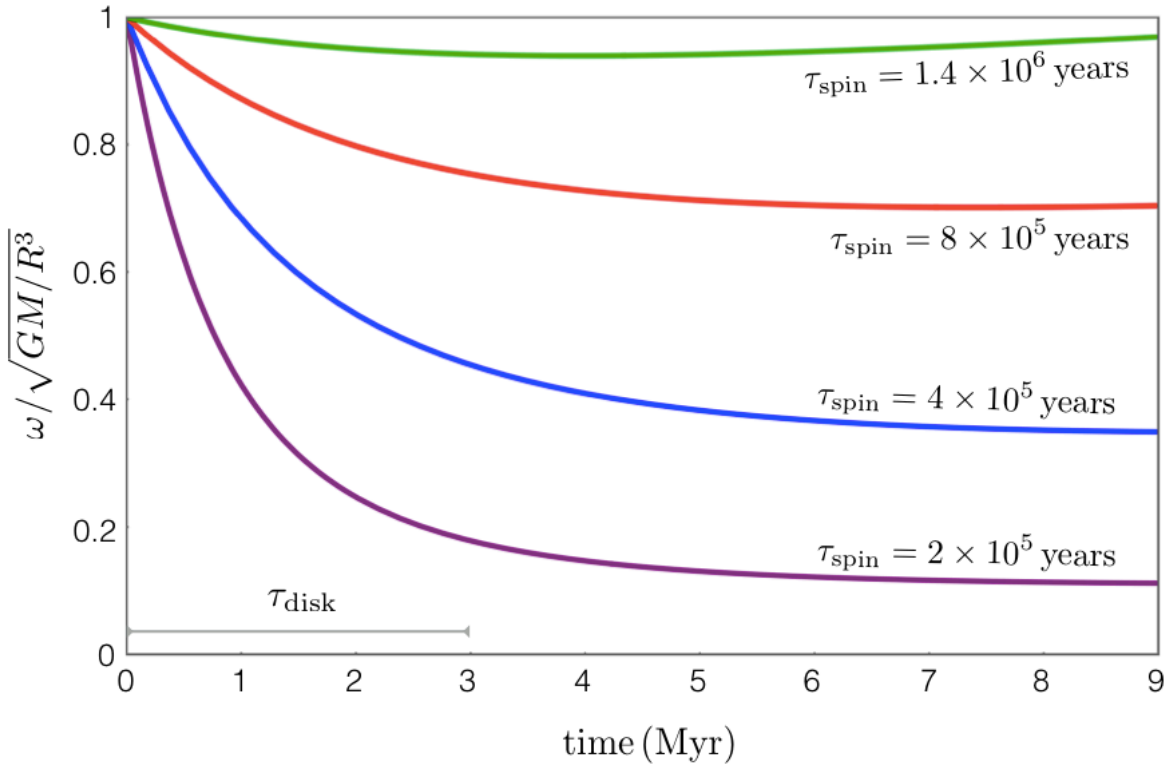

Supplementary Figure 7. Numerical solution to equation (11). A 10 M_{Jup} planet is initialized at breakup rotation (qualitatively t=0 corresponds to the conclusion of rapid gas accretion), and subsequently experiences spin-up due to gravitational contraction and accretion, as well as spin-down due to a parameterized angular momentum exchange with the circumplanetary disk.

Supplementary Table 1. *NIRSPEC K* Band Observations.

System	Pri. SpT	$m_{K,star}$ (mag)	$m_{K,pl}$ (mag)	Pl. SpT	Sep. (",AU)	M_{comp} (M_{Jup})	Age (Myr)	UT Date	AO?	No. Exp	Tot. Exp. (min)	Pl. S/N
ROXs 42B	M0	8.7	15.0	L1	1.2,140	10+/-4	3+/-2	2015/6/1	Yes	18	233	7.4
ROXs 42B	M0	8.7	15.0	L1	1.2,140	10+/-4	3+/-2	2015/6/2	Yes	6	80	4.4
GSC 6214-210	M1	9.2	14.4	L1	2.2,320	12-15	11+/-2	2015/6/3	Yes	16	240	6.0
VHS 1256-1257	M7.5	<10.4	14.7	L7	8.1,102	10-21	150-300	2015/5/7	No	14	93	11.1
OPH 90	…	…	14.9	L0	…	11+/-2	3+/-2	2015/6/4	No	8	52	16.6
USco J1608-2315	…	…	14.2	L1	…	19+/-1.5	11+/-2	2015/5/7	No	12	100	12.3
PSO J318.5-22	…	…	14.4	L7	…	8.3+/-0.5	21+/-4	2015/6/4	No	10	150	8.6
2M0355+1133	…	…	11.5	L3	…	29+/-2	120+/-10	2017/1/13	No	14	120	117.7
KPNO Tau 4	…	…	13.3	M9.5	…	25+/-2.5	2+/-1	2017/1/13	No	18	166	35.6

Supplementary Table 2. Parameters Used to Generate Atmospheric Models and Best-Fit Rotation Rates, Barycentric Radial Velocity Offsets.

System	T_{eff} (K)	log(g)	$vsini_{pl}$ (km/s)	RV_{pl} (km/s)
ROXs 42B	2100	3.81	9.5 (+2.1-2.3)	-2.3 +/- 4.0
GSC 6214-210	2188	4.05	6.1 (+4.9 - 3.8)	-7.3 +/- 4.0
VHS 1256-1257	1280	4.5	13.5 (+3.6 - 4.1)	2.1 (+1.6 - 1.7)
OPH 90	2100	3.81	8.4 (+5.5 - 5.0)	7.8 (+1.3 - 1.2)
USco 1608-2315	2442	3.95	16.3 (+2.4 - 2.5)	-4.0 (+1.1 - 1.0)
PSO J318.5-22	1325	3.7	12.0 (+3.5 - 4.4)	-6.8+/-0.7
KPNO Tau 4	2477	3.74	16.3 (+3.2 - 3.8)	17.9 (+0.7 - 0.8)
2M0355+1133	1905	4.75	14.7 (+2.1 - 2.3)	11.8 +/- 0.5

For PSO J318.5-22 T_{eff} and log(g) came from Allers et al 2016[38]. We note that the T_{eff} determined by forward modeling the spectrum of PSO J318.5-22 is higher than that inferred

from evolutionary models[22,38], suggesting that atmospheric models over-predict T_{eff}. Similarly, we adopt a higher T_{eff} for our atmospheric model for VHS 1256-1257 b than would be inferred from COND models using its mass and age, since the lower temperature models predict a significant abundance of methane that is not seen in our spectrum. All other T_{eff} and log(g) listed in this table come from COND models, where we selected temperature and surface gravity values that corresponded to masses and ages closest to inferred masses and ages of each object (Supplementary Table 1).

We determined the barycentric velocity correction for each of our RV measurements using the program barycorr[44]. We note that since we only had two AB pairs for the host star GSC 6214-210, we were not able to obtain accurate uncertainty estimates for rotation rate and RV from the MCMC analysis. We therefore adopt more robust uncertainties from our analysis of VHS 1256-1257. Rotation rates have previously been measured for 2M0355+1133[45], KPNO Tau 4[14], and PSO J318.5-22[38] with published values of 12.31+/-0.15 km/s, 10+/-2 km/s, and 17.5 (+2.3 -2.8) km/s, consistent with the measured rotation rates in this paper at 1.0σ, 1.3σ, and 1.2σ respectively. We note that the previously published spin measurements for KPNO Tau 4 and 2M0355+1133 used models including pressure broadening while our models did not, and we would expect the inclusion of pressure broadening to reduce the reported rotation rates by several km/s (see Methods section 3 for more details). RVs have previously been measured for 2M0355+1133 and PSO J318.5-22 with values of 11.92+/-0.22 km/s and -6.0 (+0.8 -1.1) km/s, consistent with our measured values at 0.2σ and 0.6σ. See Methods section 3 for a discussion of the reported RV uncertainties for companions ROXs 42B b and GSC 6214-210 b.

Supplementary Table 3. Brown Dwarf Properties, Including New Homogenous Mass Estimates and Rotation Rates From the Literature.

System	RA	Dec	SpT	Kmag (mag)	Dist. (pc)	Age (Myr)	Mass (M_{Jup})	+1σ (M_{Jup})	-1σ (M_{Jup})	*vsini*/v_{eq} (km/s)	Ref.
2M1139-3159	11 39 51.140	-31 59 21.50	M8	11.503 +/- 0.023	50+/-1.8	10+/-2	23.174	1.409	1.854	25.5	*15, 16*
2M1207-3932	12 07 33.500	-39 32 54.40	M8	11.945 +/- 0.026	50+/-1.8	10+/-2	19.916	0.925	1.187	13.7	*15, 16*
2M0537364 8-0241567	05 37 36.480	-02 41 56.70	M7	14.560 +/- 0.100	442 +/- 20	2-3	46.262	5.485	5.288	38.18	*46*
CFHT-BD-Tau 1	04 34 15.272	22 50 30.96	M7	11.849 +/- 0.018	145 +/- 15	2+/-1	54.128	6.362	10.249	7.0	*15*
CFHT-BD-Tau 2	04 36 10.387	22 59 56.03	M7.5	12.169 +/- 0.019	145 +/- 15	2+/-1	43.240	4.477	7.502	8.0	*15*

CFHT-BD-Tau 3	04 36 38.938	22 58 11.90	M7.75	12.367 +/- 0.025	145 +/- 15	2+/-1	38.652	3.544	5.619	12.0	*15*
Cha Ha 1	11 07 17.0	-77 35 54.00	M7.75	12.174 +/- 0.024	160	2	47.311	6.025	6.916	7.6	*47*
GG Tau Bb	04 32 30.25	17 31 30.90	M7.5	12.010 +/- 0.130	145 +/- 15	2+/-1	46.940	7.189	7.991	6.8	*15, 48*
IC 348 355	03 44 29.210	32 08 13.70	M8	13.499 +/- 0.035	300	1-3	47.717	4.030	5.540	45.0	*15*
IC 348 363	03 44 17.265	32 00 15.23	M8	13.695 +/- 0.038	300	1-3	43.098	3.503	4.439	14.0	*15*
IC 348 405	03 44 21.163	32 06 16.56	M8	13.910 +/- 0.100	300	1-3	38.659	3.186	3.820	45.0	*15*
KPNO Tau 5	04 29 45.680	26 30 46.81	M7.5	11.536 +/- 0.018	145 +/- 15	2+/-1	60.490	17.359	16.611	10.0	*15*
USco 130	15 59 43.665	-20 14 39.61	M7	13.075 +/- 0.034	145 +/- 15	11+/-2	56.487	16.303	23.397	14.6	*15, 16*
USco 131	16 00 19.443	-22 56 28.77	M7	13.481 +/- 0.033	145 +/- 15	11+/-2	35.950	10.238	13.445	16.0	*15*
USco DENIS 161916	16 19 16.463	-23 47 23.54	M8	13.596 +/- 0.050	145 +/- 15	11+/-2	26.305	3.760	5.949	5.0	*15*
USco DENIS 162041	16 20 41.445	-24 25 49.17	M7.5	12.902 +/- 0.019	145 +/- 15	11+/-2	60.859	21.923	18.916	16.0	*15*
2M 0537520 6-0236046	05 37 52.060	-02 36 04.60	M6.5	14.200 +/- 0.060	442 +/- 20	2-3	59.575	8.426	13.313	14.8	*46*
2M0539 1308-0237509	05 39 13.080	-02 37 50.90	M7	14.310 +/- 0.070	442 +/- 20	2-3	60.490	17.359	11.971	15.4	*46*
2M0540 0453-0236421	05 40 04.530	-02 36 42.10	M6.5	14.270 +/- 0.070	442 +/- 20	2-3	57.297	5.469	8.372	40.3	*46*
Cha Ha 12	11 05 37.5	-77 43 07.0	M6.5	11.811 +/- 0.019	160	2	76.412	17.581	24.264	25.7	*47*

GY 37	16 26 27.810	-24 26 41.82	M6	12.092 +/- 0.030	120 +/- 10	3+/-2	45.420	6.335	10.583	22.5	*15*
IC 348 478	03 44 35.937	32 11 17.51	M6.25	14.574 +/- 0.073	300	1-3	34.119	2.550	2.885	20.0	*15*
GY 141	16 26 51.284	-24 32 41.99	M8.5	13.889 +/- 0.057	120 +/- 10	3+/-2	17.953	1.877	1.961	4.9	*15, 17*
KPNO Tau 1	04 15 14.714	28 00 09.61	M8.5	13.772 +/- 0.035	145 +/- 15	2+/-1	21.394	1.867	2.558	5.5	*15*
KPNO Tau 12	04 19 01.270	28 02 48.70	M9	14.927 +/- 0.092	145 +/- 15	2+/-1	12.664	1.632	1.769	5.0	*15*
KPNO Tau 6	04 30 07.244	26 08 20.79	M8.5	13.689 +/- 0.037	145 +/- 15	2+/-1	22.047	2.023	2.473 33.032	5.0	*15*
S Ori 45	05 38 25.500	-02 48 36.00	M8.5	15.690 +/- 0.212	442 +/- 20	2-3	26.012	2.487	3.091	151	*49, 50*
TWA 5B	11 31 55.400	-34 36 29.00	M8.5	11.400 +/- 0.200	50+/-1.8	10+/-2	23.615	2.134	3.692	16.8	*15, 16*
USco DENIS 161006	16 10 06.082	-21 27 44.02	M8.5	13.768 +/- 0.056	145 +/- 15	11+/-2	23.328	2.153	2.244	7.0	*15*
OPH 90	16 27 36.59	-24 51 36.1	L0	14.85+/-0.05	120 +/- 10	3+/-2	11.243	1.545	1.670	8.4	This paper
USco 1608	16 08 27.47	-23 15 10.4	L1	14.205 +/- 0.070	145 +/- 15	11+/-2	19.157	1.226	2.128	16.4	This paper
2M0355 +1133	03 55 23.37	11 33 43.7	L3	11.526 +- 0.021	9.1+/-0.1	120+/-10	28.667	2.618	2.794	14.7	This paper
KPNO Tau 4	04 27 28.0	26 12 04.7	M9.5	13.281 +/- 0.032	145 +/- 15	2+/-1	24.970	2.794		16.3	This paper

We create this list by first identifying all brown dwarfs in the literature with spectral types later than M6, well-constrained ages typically less than 20 Myr, and measured rotation rates or rotation periods. We then derive new mass estimates using published magnitudes, spectral types, distances, and ages. Here we list median masses as well as uncertainties corresponding to the highest prior density for objects with estimated masses less than 80 M_{Jup}. Objects in italics have new measured rotation rates from our NIRSPEC program. For objects 2M05373648-0241567,

2M05375206-0236046, 2M05391308-0237509, 2M05400453-0236421, and S Ori 45, the rotation rates presented here are equatorial rotation rates determined from published photometric rotation periods; all others are projected rotation rates from measurements of rotational line broadening. The "Ref." column cites the reference where we obtained the rotation rates for each object.

Additional References

44. Wright, J. T., Eastman, J. D. Barycentric corrections at 1 cms^{-1} for precise Doppler velocities, *Publ. Astron. Soc. Pac.* **126**, 838-852 (2014).

45. Blake, C. H., Charbonneau, D., White, R. J., The NIRSPEC ultracool dwarf radial velocity survey. *Astrophys. J.* **723**, 684-706 (2010).

46. Cody, A. M., Hillenbrand, L. A., Precision photometric monitoring of very low mass σ Orionis cluster members: variability and rotation at a few Myr. *Astrophys. J., Suppl. Ser.*, **191**, 389-422 (2010).

47. Joergens, V., Guenther, E., UVES spectra of young brown dwarfs in Cha I: Radial and rotational velocities. *Astron. Astrophys.* **379**, L9-12 (2001).

48. White, R. J., Basri, G., Very low mass stars and brown dwarfs in Taurus-Auriga. *Astrophys. J.*, **582**, 1109-1122 (2003).

49. Zapatero Osorio, M. R., Caballero, J. A., Bejar, V. J. S., Rebolo, R., Photometric variability of a young, low-mass brown dwarf. *Astron. Astrophys.*, **408**, 663-673 (2003)

50. Zapatero Osorio, M. R. *et. al.*, Dynamical masses of the binary brown dwarf GJ 569 Bab. *Astrophys. J.,* **615**, 958-971 (2004).